Cancer Cell
Article

Aneuploidy Acts Both Oncogenically and as a Tumor Suppressor

Beth A.A. Weaver,[1] Alain D. Silk,[1] Cristina Montagna,[2,3] Pascal Verdier-Pinard,[4,5] and Don W. Cleveland[1,*]
[1] Ludwig Institute for Cancer Research and Department of Cellular and Molecular Medicine, University of California, San Diego, 9500 Gilman Drive, La Jolla, CA 92093, USA
[2] Department of Pathology
[3] Department of Molecular Genetics
[4] Department of Molecular Pharmacology
[5] Department of OB/GYN and Women's Health
Albert Einstein College of Medicine, Bronx, NY 10461, USA
*Correspondence: dcleveland@ucsd.edu
DOI 10.1016/j.ccr.2006.12.003

SUMMARY

An abnormal chromosome number, aneuploidy, is a common characteristic of tumor cells. Boveri proposed nearly 100 years ago that aneuploidy causes tumorigenesis, but this has remained untested due to the difficulty of selectively generating aneuploidy. Cells and mice with reduced levels of the mitosis-specific, centromere-linked motor protein CENP-E are now shown to develop aneuploidy and chromosomal instability in vitro and in vivo. An increased rate of aneuploidy does drive an elevated level of spontaneous lymphomas and lung tumors in aged animals. Remarkably, however, in examples of chemically or genetically induced tumor formation, an increased rate of aneuploidy is a more effective inhibitor than initiator of tumorigenesis. These findings reveal a role of aneuploidy and chromosomal instability in preventing tumorigenesis.

INTRODUCTION

It was well known a century ago that aneuploidy is a common characteristic of cancer cells. Based on this correlation, and his observations of the pathological consequences of aneuploidy in fertilized sea urchin oocytes, Theodor Boveri proposed in 1902 and 1914 that aneuploidy drives tumorigenesis (Boveri, 1902, 1914). With the subsequent discovery of oncogenes and tumor suppressors, Boveri's hypothesis, now known as the aneuploidy hypothesis, has remained controversial. Aneuploidy-inducing carcinogens do drive tumorigenesis, but these have subsequently been shown to be mutagenic as well (Li et al., 1997; Quintanilla et al., 1986). On the other hand, human cells have been reported to become transformed without widespread genetic changes, including aneuploidy, due to coexpression of the SV40 large T antigen, the telomerase catalytic subunit hTERT, and oncogenic ras (Hahn et al., 1999; Zimonjic et al., 2001). However, later examination proved 70% of these cells to have a nondiploid karyotype (Li et al., 2000).

Aneuploidy caused by reduction in one of three essential components of the mitotic checkpoint, Mad2 (Babu et al., 2003; Baker et al., 2004; Michel et al., 2001), Bub3 (Babu et al., 2003; Baker et al., 2004; Michel et al., 2001), or BubR1 (Babu et al., 2003; Baker et al., 2004; Michel et al., 2001), has been implicated in tumorigenesis. The mitotic checkpoint, also known as the spindle assembly checkpoint, is a major mitotic cell-cycle control mechanism that prevents missegregation of even single chromosomes by delaying advance to anaphase until the centromeres of all chromosomes have attached to

SIGNIFICANCE

Aneuploidy is a remarkably common feature of human cancers and has been proposed to drive tumorigenesis, to contribute to tumor progression, or to be completely benign. Aneuploidy due to continuous missegregation of random, individual chromosomes is now shown to promote spontaneous tumorigenesis in aged animals, but only at a modest frequency. Strikingly, however, aneuploidy and chromosomal instability due to reduction in the mitosis-specific motor CENP-E actually inhibits tumorigenesis in the presence of additional genetic damage. These data advance a paradigm in which low levels of chromosomal instability promote tumor initiation and progression, but higher levels are protective and suggest that highly aneuploid, chromosomally unstable tumors may exhibit enhanced sensitivity to aneugenic or DNA-damaging drugs.

spindle microtubules (Cleveland et al., 2003). Mice heterozygous for the essential mitotic checkpoint protein Mad2 develop spontaneous, benign, self-limiting lung adenomas with long latencies (18–20 months; Michel et al., 2001). *Bub3*$^{+/-}$ mice do not show an increase in spontaneous tumorigenesis but do exhibit a trend toward increased sensitivity to chemically induced lung tumors (Babu et al., 2003; Baker et al., 2006; Kalitsis et al., 2005), while mice with reduced levels of BubR1 exhibit increased susceptibility to tumors induced by carcinogens (Baker et al., 2006; Dai et al., 2004) or mutations in the adenomatous polyposis coli tumor suppressor (Rao et al., 2005). Moreover, germline mutations in the gene encoding BubR1 have recently been identified in patients with the inherited cancer-prone syndrome mosaic variegated aneuploidy (Hanks et al., 2004; Matsuura et al., 2006).

Nevertheless, no conclusion can be drawn from these apparent correlations between diminished mitotic checkpoint signaling and tumorigenesis, since each of these mitotic checkpoint contributors is also present throughout interphase and is known to participate in cellular functions other than chromosome segregation. Mad2, for example, is bound to the nuclear envelope and nuclear pores (Campbell et al., 2001; Iouk et al., 2002) and has been implicated both in the DNA replication checkpoint (Sugimoto et al., 2004) and in promoting gross chromosomal rearrangements in yeast (Myung et al., 2004). Bub3 interacts with histone deacetylases, acts to repress transcription (Yoon et al., 2004), and contributes to chromosomal rearrangements (Myung et al., 2004). BubR1 has been shown to be involved in numerous cellular processes including premature aging (Baker et al., 2004), apoptosis (Baek et al., 2005; Kim et al., 2005; Shin et al., 2003), fertility (Baker et al., 2004), megakaryopoiesis (Wang et al., 2004), gross chromosomal rearrangements (Myung et al., 2004), and the response to DNA damage (Fang et al., 2006). Thus, the ability of aneuploidy per se to drive tumorigenesis remains untested by efforts with reduced levels of any of these multifunctional proteins. Rather, the hypothesis that aneuploidy promotes tumorigenesis remains unproven, as are alternative views that aneuploidy is merely a benign side effect of transformation or a contributor to tumor progression but not to tumor initiation (Marx, 2002).

We report here that cells and animals with reduced levels of *CEN*tromere-associated *P*rotein-*E* (CENP-E) become aneuploid due to the random missegregation of one or a few chromosomes at high rates in the absence of DNA damage. CENP-E is an essential, mitosis-specific, cell-cycle-regulated motor that accumulates primarily in late G2 and is used in mitosis and then degraded at the end of mitosis as quantitatively as is cyclin B (Brown et al., 1994). A large (~312 kDa in human) kinesin-like motor protein, CENP-E is conserved in all but the simplest metazoans and plays at least two critical functions during mitosis (Putkey et al., 2002; Wood et al., 1997; Yen et al., 1991; Yucel et al., 2000). First, it participates in making and/or maintaining the interactions between chromosomes and the microtubules of the mitotic spindle (McEwen et al., 2001; Putkey et al., 2002). Second, CENP-E serves a bifunctional role in the mitotic checkpoint. It first stimulates mitotic checkpoint signaling by serving as a "cyclin-like" activator of BubR1 kinase activity (Mao et al., 2003; Weaver et al., 2003) and then turns off production of the BubR1-dependent "wait anaphase" inhibitor when all chromosomes have made appropriate attachments to spindle microtubules (Mao et al., 2005).

We have exploited the property that cells and mice with reduced CENP-E generate high rates of aneuploidy in the absence of other observable defects to test the hypotheses that aneuploidy (1) drives tumorigenesis, (2) is benign, or (3) promotes tumor progression but not initiation. We find that aneuploidy due to the repetitive missegregation of one or a few whole chromosomes contributes to transformation in vitro and causes a modest increase in spontaneous spleen and lung tumors in vivo. Surprisingly, in examples of chemically or genetically induced tumor formation, an increased rate of aneuploidy can be a more effective inhibitor than initiator of tumorigenesis.

RESULTS

CENP-E$^{+/-}$ Cells Rapidly Develop Aneuploidy In Vitro

Primary mouse embryo fibroblasts (MEFs) were prepared from mice containing one normal and one disrupted CENP-E allele. Immunoblotting for CENP-E revealed that CENP-E$^{+/-}$ cells contained the expected ~50% of the CENP-E level present in comparable wild-type cells (Figure 1A; Figures S1A and S1B in the Supplemental Data available with this article online), and this reduced level remained associated with kinetochores (Figure 1B, upper panel). As expected, CENP-E protein was undetectable in interphase cells (Figure 1B, lower panel). Reduction in CENP-E produced cells in which one or a few chromosomes were unable to make stable attachments to microtubules and remained misaligned near one of the spindle poles (Figure 1C, lower panel). These misaligned chromosomes subsequently become missegregated in one-quarter of CENP-E$^{-/-}$ cells (Weaver et al., 2003). As an initial measure of the fidelity of chromosome transmission in CENP-E$^{+/-}$ fibroblasts, chromosome spreads (also known as metaphase spreads) were prepared from cells arrested in mitosis by drug-induced microtubule disassembly (Figure 1D). The number of chromosomes per spread was determined, and cells were scored as diploid (2n = 40), tetraploid (4n = 80), or aneuploid. Although aneuploidy increased with time in culture for both genotypes, primary MEFs with reduced CENP-E were significantly more aneuploid than wild-type MEFs at all time points (Figure 1E).

Examination of the absolute number of chromosomes per cell revealed two populations in each genotype (n = 100 spreads from each of three independent experiments). While most of the cells were diploid or near-diploid, a subset of the population (~2%–20%, increasing with time in culture) contained a tetraploid or near-tetraploid number of chromosomes, consistent with failure of cytokinesis in a prior mitosis. The percentage of cells that failed

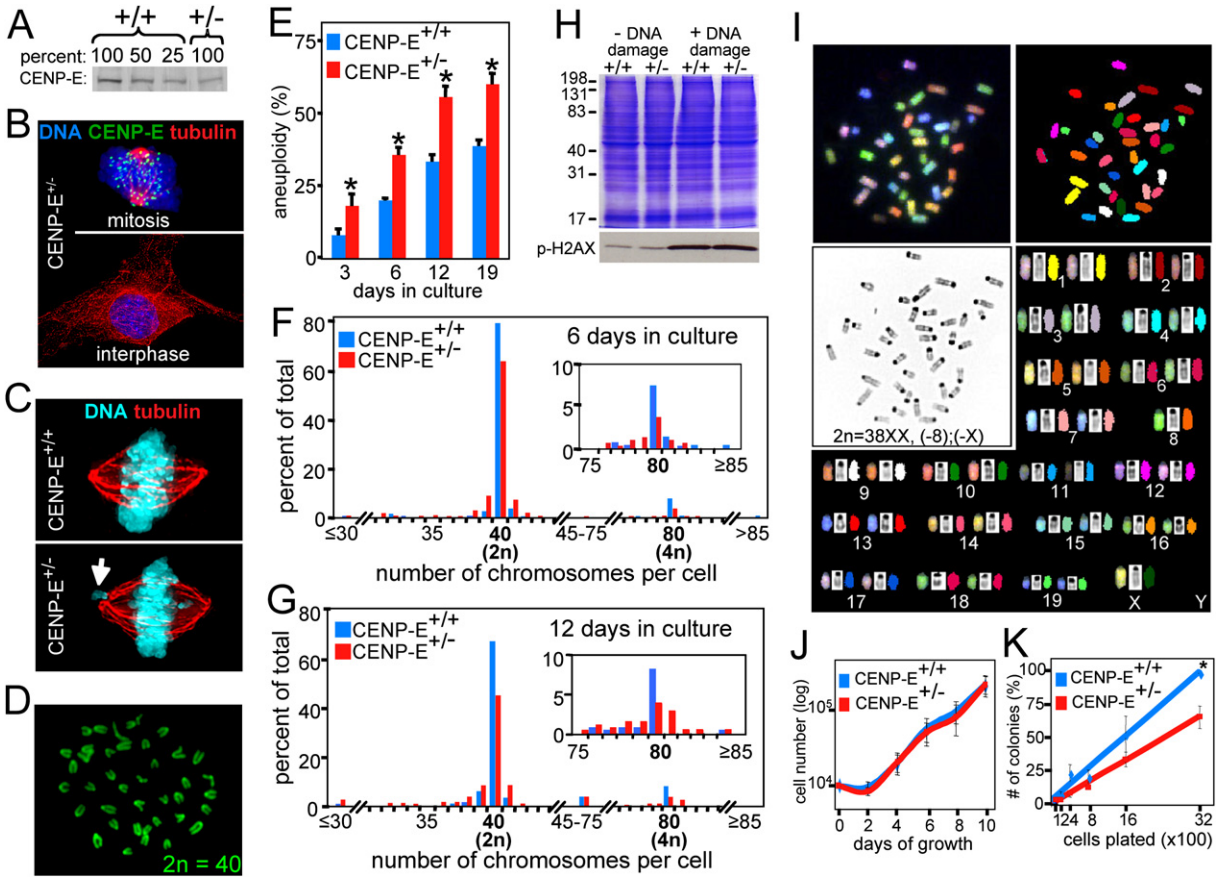

Figure 1. CENP-E$^{+/-}$ MEFs Rapidly Develop Aneuploidy In Vitro

(A) Immunoblot showing that CENP-E protein levels are reduced by ≥50% in CENP-E$^{+/-}$ primary MEFs as compared to CENP-E$^{+/+}$ MEFs.

(B) CENP-E (green) localizes to kinetochores (which assemble at the centromeric regions of mitotic chromosomes) during mitosis. CENP-E is undetectable during interphase. Tubulin, red; DNA, blue.

(C) Upper panel; normal metaphase alignment of chromosomes in a wild-type cell. Lower panel; CENP-E$^{+/-}$ cell containing a misaligned chromosome near the spindle pole (arrow). DNA, blue; tubulin, red.

(D) Representative chromosome (metaphase) spread prepared from a primary MEF. DNA was visualized with DAPI. Replicated chromosomes (sister chromatids) appear as V shapes because the centromeres are very close to the telomeres (acrocentric). Diploid murine cells contain 40 replicated chromosomes when arrested in mitosis, as these are.

(E) CENP-E$^{+/-}$ cells are significantly more aneuploid than wild-type cells. The percentage of aneuploid cells in primary MEFs grown in culture for 3–19 days is graphed as mean ± SD. Aneuploidy increases with time in culture in both genotypes, but CENP-E$^{+/-}$ cells are significantly more aneuploid at all time points. n = 100 spreads from each of three independent experiments. *p < 0.05.

(F and G) Absolute chromosome numbers of primary MEFs grown in culture for 6 (F) or 12 (G) days, showing the presence of both diploid (or near-diploid) and tetraploid (or near-tetraploid) populations. The insets show an enlarged view of the near-tetraploid populations. n = 100 spreads from each of three independent experiments.

(H) Immunoblot showing histone H2AX is phosphorylated (a marker of DNA damage) at similar levels in wild-type and CENP-E$^{+/-}$ cells. DNA damage was induced by 6.5 hr treatment with 0.5 μM doxorubicin. Coomassie is shown as a loading control.

(I) Spectral karyotyping of a CENP-E$^{+/-}$ primary cell showing numerical but not structural aberrations. Fifteen cells from two independent animals were examined.

(J) Population growth rates of CENP-E$^{+/+}$ and CENP-E$^{+/-}$ cells are indistinguishable. Data are graphed as mean ± SEM.

(K) Colony-forming assay. Individual CENP-E$^{+/-}$ cells are significantly less viable than CENP-E$^{+/+}$ cells. Data are presented as mean ± SEM. *p < 0.05.

cytokinesis was identical in cells with normal and reduced levels of CENP-E. However, in both populations, the range of chromosome numbers in CENP-E$^{+/-}$ cells was wider than the range of chromosome numbers found in wild-type cells, consistent with missegregation of one or a few chromosomes per division (Figures 1F and 1G).

CENP-E accumulates in late G2, localizes to kinetochores (which assemble at the centromeric region of mitotic chromosomes) during all phases of mitotic chromosome movement, and is degraded during mitotic exit (Brown et al., 1994). Even at peak levels, CENP-E accumulates only to levels sufficient to provide 50 molecules per kinetochore (Brown et al., 1994). It is undetectable in nondividing tissues (Figure S1C) and throughout most of interphase in cycling cells (Figure 1B, lower panel). Beyond its kinesin-like motor domain, it has no catalytic

motifs, such a kinase domain, that would permit it to provide a significant role when present at trace amounts. CENP-E is therefore highly unlikely to participate in cellular functions other than those in mitosis. Consistent with this, DNA damage, as assessed by levels of phosphorylated histone H2AX, is not elevated in untreated CENP-E$^{+/-}$ cells (Figure 1H, left lanes). However, DNA damage caused by treatment with the DNA topoisomerase II inhibitor doxorubicin induced phosphorylation of H2AX to a similar extent in both wild-type and CENP-E$^{+/-}$ MEFs, indicating that the DNA damage response remains intact in cells with reduced CENP-E (Figure 1H, right lanes). Sequencing of the p53 gene in CENP-E$^{+/-}$ cells revealed no mutations, as expected. Furthermore, spectral karyotyping (SKY) revealed that chromosomes in CENP-E$^{+/-}$ cells do not exhibit structural rearrangements, including translocations, insertions, and deletions [Figure 1I, karyotype 38XX, (−8);(−X)]. Therefore, although a role for CENP-E outside of mitosis cannot be formally excluded, no evidence supports such a hypothetical role, and there is substantial evidence against one. We conclude that CENP-E heterozygosity induces near-diploid aneuploidy and chromosomal instability in the absence of other observable defects.

Aneuploidy Contributes to Transformation In Vitro

The ability of aneuploidy to contribute to tumorigenicity was examined in primary MEFs, as well as in immortalized MEFs prepared in two different ways. First, we exploited the property that MEFs that are homozygous null for the tumor suppressor p19/ARF are immortal under standard culture conditions, since p19/ARF is essential for cellular senescence in mouse cells (Kamijo et al., 1997). MEFs that were null for p19/ARF and heterozygous for CENP-E were generated from embryos of the corresponding genotypes, after two rounds of mating of mice containing disrupted p19/ARF and/or CENP-E alleles. Second, immortalized MEFs were prepared by transfecting CENP-E$^{+/+}$ or CENP-E$^{+/-}$ primary MEFs with the SV40 large T antigen, one of three cooperating transforming antigens in the SV40 genome. It should be noted that, although SV40 large T can transform some immortalized cell lines autonomously, it is incapable of independently transforming primary MEFs (Rundell and Parakati, 2001). Interestingly, immortalization of MEFs by SV40 large T is accompanied by conversion to tetraploidy (data not shown).

Examination of the in vitro characteristics of chromosomally unstable CENP-E$^{+/-}$ cells relative to their normal counterparts revealed no differences in the growth rate (Figure 1J). Similarly, in p19/ARF null cells or those immortalized with SV40 large T antigen, growth rates were indistinguishable between cells generating higher rates of aneuploidy from reduction of CENP-E and those with normal CENP-E content (Figure S2A). Since homozygous loss of individual autosomes would be expected to generate a proportion of nonviable progeny, the unchanged doubling times indicate that rates of chromosome loss are too modest to generate a high proportion of such lethal losses in the overall cell population. However, assessment of colony growth from single cells revealed a clear difference in the proportion of surviving colonies, with viability of CENP-E$^{+/-}$ cells of all three cell types clearly reduced compared to CENP-E$^{+/+}$ cells (Figure 1K; Figure S2B).

Aneuploid CENP-E$^{+/-}$ cells were also tested for characteristics of transformed cell growth. Primary MEFs, as well as MEFs immortalized from homozygous loss of p19/ARF or transfection of the SV40 large T antigen, were analyzed for the ability to form foci on plastic. Staining of confluent cells with crystal violet revealed that, in all three cell types, aneuploidy due to CENP-E heterozygosity strongly enhanced the ability to form foci (Figures 2A and 2B), some of which grew large enough to be visible to the naked eye (Figure S3A). Immunofluorescence staining revealed these foci to be densely packed three-dimensional masses of cells containing normal, abnormal, dying, and dividing cells (Movie S1). Immortalized CENP-E$^{+/-}$ cells that did not form foci grew to higher saturation densities than corresponding CENP-E$^{+/+}$ cells (Figures S3C–S3D).

The influence of aneuploidy on anchorage-independent growth in soft agar was also examined. Neither primary CENP-E$^{+/-}$ nor CENP-E$^{+/+}$ MEFs grew in soft agar, irrespective of passage number (Figure 2C, upper panels). A similar situation was observed for early-passage p19/ARF null cells (Kamijo et al., 1999, and data not shown). Late-passage ($\geq$30 passages) p19/ARF null, CENP-E$^{+/+}$ MEFs did exhibit limited growth in soft agar, but CENP-E heterozygosity eliminated this in cells derived from most p19/ARF null embryos (Figure 2C, center panels). However, in a minority of p19/ARF null cells, CENP-E heterozygosity greatly facilitated growth in soft agar (Figure 2C, center panels, inset), presumably as a consequence of increased random chromosome missegregation producing a rare aneuploid genotype that cooperates with loss of p19/ARF to transform cells. Similarly, in cells expressing SV40 large T, CENP-E heterozygosity reduced the number of microscopic colonies formed in soft agar relative to CENP-E$^{+/+}$ cells (Figure S3E), while the very small number of macroscopic colonies (with high growth rates) increased significantly in cells with reduced CENP-E (Figure S3F). These latter colonies grew substantially larger and much more rapidly than similar colonies of CENP-E$^{+/+}$ cells (Figure 2C, lower panels).

Aneuploidy Contributes to Tumorigenicity In Vivo

To test if increased chromosomal loss or gain would affect tumorigenicity, primary MEFs, p19/ARF null MEFs, and SV40 large T immortalized MEFs that had normal or reduced CENP-E levels (and that had not been passaged through soft agar) were tested for the ability to form tumors when injected into nude mice. Animals injected with primary MEFs and low-passage immortalized MEFs did not form tumors at the injection site. Nor did animals injected with late-passage p19/ARF cells with normal levels of CENP-E, even 3 months after injection (n = 6). The majority of p19/ARF null, CENP-E$^{+/-}$ cells also did not form tumors in nude mice (n = 6). However, 19 of 19 mice injected with transformed p19/ARF null, CENP-E$^{+/-}$ cells (as scored by the ability to grow in soft agar) formed

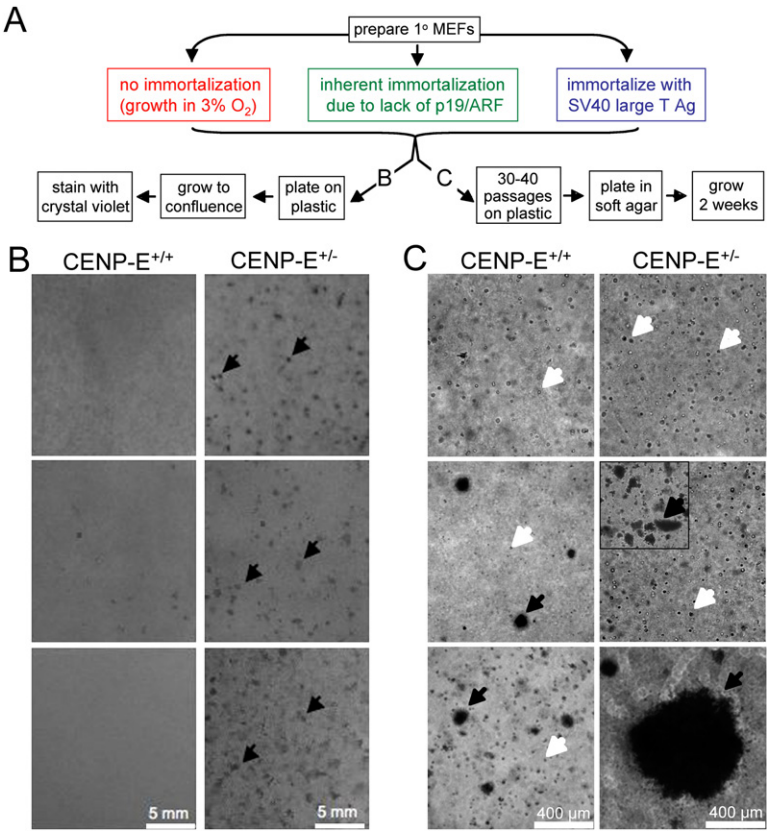

Figure 2. Aneuploid CENP-E$^{+/-}$ Cells Exhibit Characteristics of Transformed Cell Growth

(A) Schematic of the experiment.

(B) CENP-E heterozygosity results in focus formation on plastic in (top) primary MEFs, (middle) MEFs immortalized due to homozygous loss of p19/ARF, and (bottom) MEFs immortalized due to transfection with SV40 large T antigen. Foci appear as puncta of enriched dye staining (arrows) and are indicative of loss of contact inhibition.

(C) CENP-E heterozygosity facilitates growth in soft agar in (bottom) SV40 large T-expressing cells and (middle, inset: shown at one-fourth the magnification of the main panels) in a subset of p19/ARF$^{-/-}$ cells. However, (middle) in a majority of p19/ARF null cells, CENP-E heterozygosity abrogates the limited growth in soft agar observed in late-passage p19/ARF$^{-/-}$ MEFs. (Top) Primary CENP-E heterozygous and CENP-E wild-type fibroblasts did not form colonies. Late-passage cells (>passage 30) were plated in soft agar and monitored for anchorage-independent growth. Early-passage cells did not give rise to colonies in soft agar (data not shown). White arrows indicate single cells that did not grow. Black arrows indicate colonies.

tumors at the injection site with a very short latency (~1–2 weeks; Figure 3A). Ten of ten mice injected with high-passage ($p \geq 45$) CENP-E$^{+/-}$ MEFs expressing SV40 large T formed tumors at the injection site with a latency between 1 and 6 weeks. None of the mice injected with CENP-E$^{+/+}$ MEFs immortalized with SV40 large T formed tumors at the injection site within the same time frame (Figure 3B). (One of 12 mice injected with late-passage CENP-E$^{+/+}$ cells expressing SV40 large T did form a tumor at the injection site, but it took 12 weeks to form, twice the length of the longest latency of tumors formed by CENP-E$^{+/-}$ cells expressing SV40 large T.)

Histological examination of the tumors from p19/ARF$^{-/-}$, CENP-E$^{+/-}$, or CENP-E$^{+/-}$ cells expressing SV40 large T revealed each to be a fibromyosarcoma, as expected for derivation from the injected MEFs. This conclusion was confirmed by genotyping, which showed the continued presence of one wild-type and one null allele (Figure S4; data not shown). Cell lines were successfully isolated from a subset of the tumors, and chromosome spreads from these lines were examined (Figures 3C and 3D). The tumor cells exhibited a wide range of chromosome numbers, indicative of the expected chromosomal instability.

Age-Dependent Increases in Aneuploidy in Animals with Reduced CENP-E

Aneuploidy rates were assessed in three different tissue types from mice with normal or reduced levels of CENP-E. Chromosome spreads from peripheral blood lymphocytes collected from mice from 2 to 20 months of age were evaluated. Age-dependent accumulation of aneuploidy in lymphocytes was observed in both genotypes, but at all ages CENP-E$^{+/-}$ animals contained a significantly higher percentage of aneuploid cells. Notably, a majority of CENP-E$^{+/-}$ lymphocytes were aneuploid by 10 months of age (Figure 4A).

Similarly, analysis of chromosome spreads from splenocytes of 8-month-old animals revealed 35% of splenocytes from CENP-E$^{+/-}$ animals to have a nondiploid number of chromosomes, as compared to 10% of splenocytes from age-matched CENP-E$^{+/+}$ littermates (Figure 4B). The distribution of chromosomes per cell was not symmetrically centered on 40 but was skewed toward chromosome loss. Chromosome numbers of 25–39 were common, while chromosome numbers above 40 were only rarely observed. More than 42 chromosomes were not detected in mice under 12 months of age (Figures 4C–4F). No tetraploid cells were detected in splenocytes or in lymphocytes from peripheral blood (Figure 4; data not shown), unlike in the MEFs grown in vitro. This skewing toward chromosome loss was consistently observed in every sample of splenocytes and peripheral blood lymphocytes (Figures 4C–4F; data not shown) and is consistent with previous observations in normal developing neuronal precursors (Kaushal et al., 2003; McConnell et al., 2004; Rehen et al., 2001; Yang et al., 2003).

Finally, aneuploidy in colon sections was determined using interphase *f*luorescence *i*n *s*itu *h*ybridization

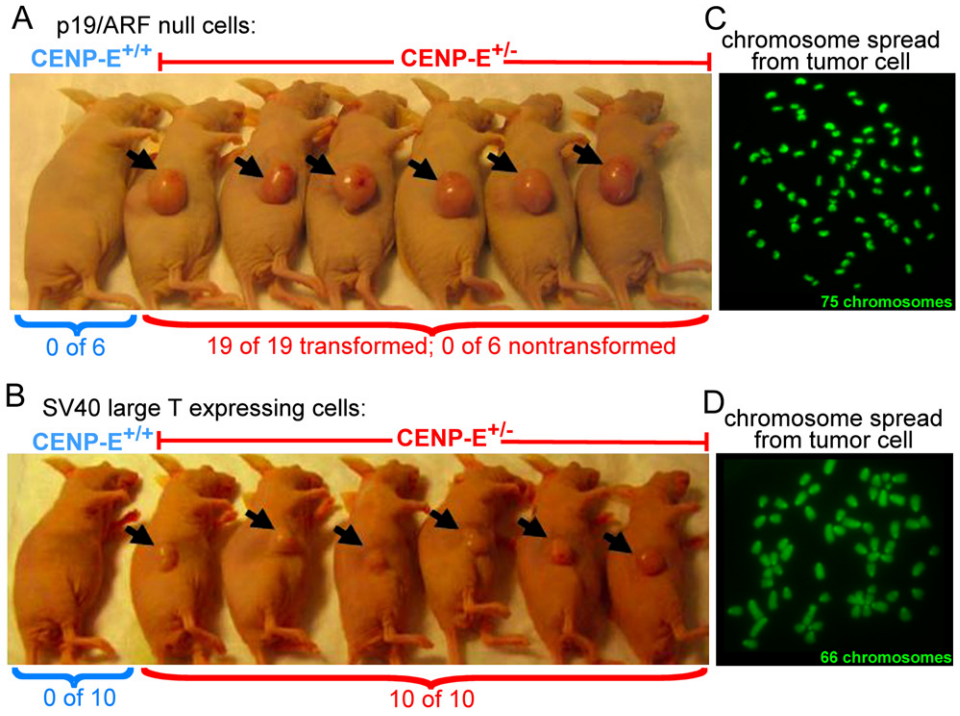

Figure 3. Aneuploidy Due to CENP-E Heterozygosity Contributes to Tumorigenicity

Cells that had not been passaged through soft agar were injected into nude mice.

(A) Nude mice injected with late-passage p19/ARF$^{-/-}$, CENP-E$^{+/-}$ cells that grow in soft agar form tumors at the injection site (arrows), while mice injected with late-passage p19/ARF$^{-/-}$, CENP-E$^{+/-}$ cells that abrogate growth in soft agar or late-passage p19/ARF$^{-/-}$, CENP-E$^{+/+}$ cells do not form tumors.

(B) Nude mice injected with CENP-E$^{+/-}$ cells expressing SV40 large T form tumors at the injection site (arrows), but mice injected with CENP-E$^{+/+}$ cells expressing SV40 large T do not.

(C and D) Chromosome spreads prepared from p19/ARF$^{-/-}$, CENP-E$^{+/-}$ tumor cells (C) (n = 30) and CENP-E$^{+/-}$ SV40 large T-expressing tumor cells (D) (n = 100). The number of chromosomes in the spread shown is noted in the bottom right-hand corner.

(FISH). Sections from 19-month-old animals were hybridized with FISH probes against chromosome 2 or the Y chromosome. In both cases, colon cells from CENP-E$^{+/-}$ mice were significantly more aneuploid (~4- to 6-fold) than colon cells from age-matched wild-type animals (Figures 5A and 5B), reaching 17%–20% of total cells for each of the chromosomes examined.

Despite elevated levels of aneuploidy in all cell types examined, CENP-E$^{+/-}$ animals were overtly normal. Both male and female animals were viable and fertile and produced normal litter sizes (6.2 ± 2.5 mice per litter; n = 20 litters). At all ages, CENP-E$^{+/-}$ animals maintained healthy body weights (Figure S5A), and weights of individual organs were not significantly different from their wild-type littermates (Figures S5B–S5D).

Aneuploidy Drives Tumorigenesis In Vivo

To determine if the elevated aneuploidy generated in vivo in mice with reduced CENP-E can drive tumorigenesis, cohorts of wild-type and CENP-E$^{+/-}$ animals were aged to 19–21 months and examined for the development of spontaneous tumors. Lymphomas of the spleen were detected in 10% of CENP-E$^{+/-}$ mice, while none of the wild-type mice had similar tumors, a difference that was statistically significant ($p = 0.0402$; Figure 6A). Lymphomas exhibited effacement of lymphoid follicles and replacement of splenic architecture with a monoclonal proliferation of neoplastic cells (Figure 6C; Figures S6C–S6F). Malignant cells displayed an elevated nucleus to cytoplasm ratio and contained large nuclei (4- to 6-fold larger than normal lymphocytes) with prominent nucleoli (Figure 6E).

Additionally, a statistically significant 3-fold increase in lung tumors in the aged CENP-E$^{+/-}$ versus normal littermates was observed ($p = 0.0492$; Figure 6A). Histological examination identified these as pulmonary adenomas (Figures 6G–6I). Thus, aneuploidy caused by elevated rates of whole-chromosome missegregation in CENP-E$^{+/-}$ animals validates Boveri's initial hypothesis: aneuploidy can indeed promote tumorigenesis in the absence of other observable defects.

Aneuploidy Inhibits Tumorigenesis in Tissues Prone to Tumor Formation

Liver tumors were the most common neoplasms observed in our wild-type mice, with 14% of wild-type animals having one or more. Despite increases in lung adenomas and splenic lymphomas, widespread aneuploidy was accompanied by a 50% decrease of spontaneous liver

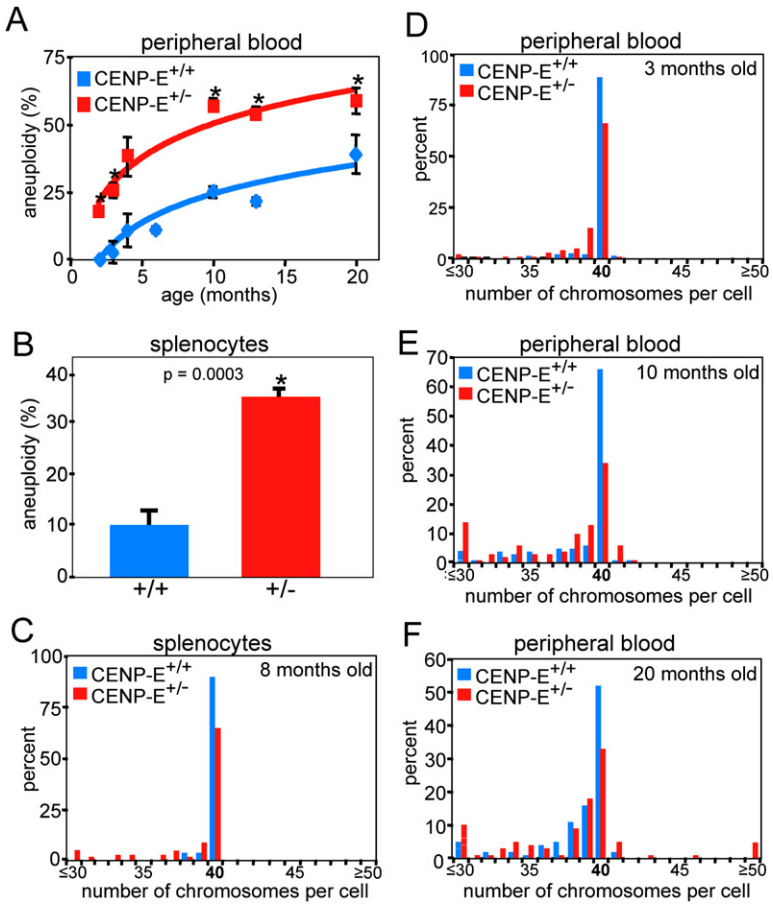

Figure 4. In Vivo Aneuploidy in Lymphocytes and Splenocytes from Reduced CENP-E

(A) CENP-E$^{+/-}$ mice contain high levels of aneuploid cells that are not eliminated from the cycling population. Aneuploidy, scored by preparing chromosome spreads from peripheral blood cells (n = 50 from each of two independent experiments), increases with age. Data are shown as the mean ± SD.

(B) Spleen cells from CENP-E$^{+/-}$ animals have elevated levels of aneuploidy (as scored by chromosome spreads). Data are shown as the mean ± SD.

(C–F) The number of chromosomes per cell in splenocytes from 8-month-old animals (C) or peripheral blood lymphocytes from animals 3 months (D), 10 months (E), and 20 months (F) of age is shown. No spreads containing fewer than 24 or more than 57 chromosomes were counted.

tumors in aged CENP-E$^{+/-}$ animals (to 7%; Figure 7A; Table S1). None of these animals had more than one. Additionally, the tumors in the wild-type livers were significantly larger than the tumors observed in the CENP-E$^{+/-}$ animals (Figure 7B). Although the increase in the number of liver tumors identified in wild-type animals versus CENP-E$^{+/-}$ animals did not quite reach statistical significance (p = 0.0578), the size of the tumors observed in wild-type animals versus those in CENP-E$^{+/-}$ animals was significantly different (p = 0.0037). Interestingly, in addition to the polyploidy commonly identified in hepatocytes, ~20% of wild-type murine liver cells missegregate one or more chromosomes at each mitosis (Putkey et al., 2002). Thus, increasing aneuploidy further by reduction in CENP-E actually inhibits the growth of spontaneous tumors in the liver.

To determine whether aneuploidy due to recurrent losses or gains of one or a few chromosomes affected tumor initiation or progression in tumors provoked by exposure to a well-characterized carcinogen, 7,12-dimethylbenz[a]anthracene (DMBA), thirty-eight animals were given a single dose of DMBA at postnatal day 3–5. The animals were sacrificed at 8 months of age and examined for tumors. Forty percent of the wild-type animals harbored a single lung tumor. An additional wild-type animal that did not develop a lung tumor contained one ovarian and two mammary tumors. Surprisingly, lung tumors were identified in a smaller portion of the CENP-E$^{+/-}$ animals (31%; Figure 7C), and these tumors also showed a trend toward reduced size (0.30 ± 0.06 mm^3 in wild-type versus 0.20 ± 0.11 mm^3 in CENP-E$^{+/-}$). No tumors were identified in any other organs in the CENP-E$^{+/-}$ mice. The apparent reduction in tumorigenesis observed in CENP-E$^{+/-}$ animals after DMBA treatment did not reach statistical significance (p = 0.1255). However, aneuploidy due to CENP-E heterozygosity did not accelerate tumor initiation or progression after treatment with this carcinogen.

The effect of aneuploidy on tumors initiated by the complete absence of a tumor suppressor was also tested. Two rounds of mating produced CENP-E$^{+/-}$ animals that were deficient for the p19/ARF tumor-suppressor gene, as well as p19/ARF$^{-/-}$, CENP-E$^{+/+}$ littermates. p19/ARF$^{-/-}$ animals develop malignant cancers, predominantly sarcomas and lymphomas. Adding elevated rates of single-chromosomal loss to tumors initiated by absence of the p19/ARF tumor suppressor had a striking and unexpected effect on survival. Elevated aneuploidy increased the average tumor-free survival of these animals by a highly significant 93 days (Figure 7D; p = 0.0079), with all but one animal exhibiting a substantially longer tumor latency, consistent with CENP-E heterozygosity abrogating the limited growth in soft agar observed in late-passage

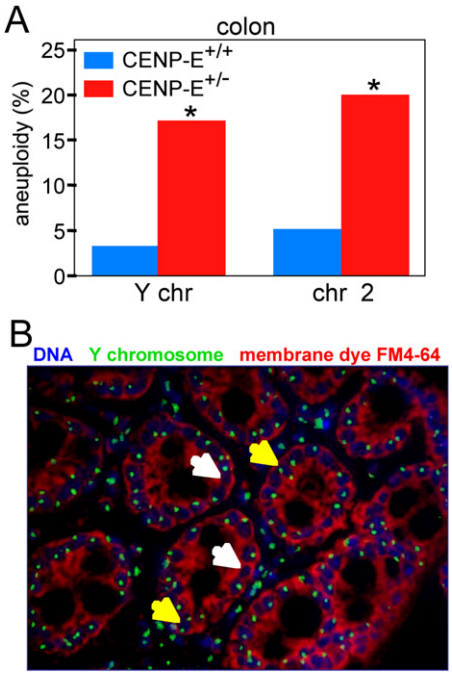

Figure 5. CENP-E$^{+/-}$ Mice Develop Aneuploidy In Vivo
(A and B) Colon cells from CENP-E$^{+/-}$ animals have elevated levels of aneuploidy. (A) Quantitation of aneuploidy (loss and gain) of the Y chromosome and chromosome 2 in 19-month-old animals. *p < 0.05. (B) Interphase FISH image of a 6 μm tissue section from the colon of a 19-month-old animal. DNA, blue; membrane dye FM4-64, red; FISH paint probe to the entire Y chromosome, green.

p19/ARF$^{-/-}$, CENP-E$^{+/+}$ cells. Nevertheless, one p19/ARF$^{-/-}$, CENP-E$^{+/-}$ animal developed a tumor with a very short latency (62 days), consistent with the in vitro data indicating that in rare instances aneuploidy can enhance tumorigenicity caused by loss of the p19/ARF tumor suppressor. p19/ARF$^{-/-}$, CENP-E$^{+/-}$ animals did not exhibit a shift in the tumor spectrum from lymphomas to solid tumors. Moreover, we confirmed that tumors in p19/ARF$^{-/-}$, CENP-E$^{+/-}$ animals remained heterozygous for CENP-E (Figure S4). Thus, aneuploidy from whole-chromosome loss (or gain) can strongly delay in vivo tumorigenesis after loss of the p19/ARF tumor-suppressor gene.

DISCUSSION

By reduction in a mitotic motor that is a component of mitotic checkpoint signaling, we have demonstrated that increased rates of single-chromosomal aneuploidy in the absence of other observable defects can enhance transformation in culture and spontaneous tumorigenesis during aging, while diminishing tumor formation initiated by loss of the p19/ARF tumor suppressor. These outcomes provide a direct test of the 100-year-old hypothesis that aneuploidy, a salient characteristic of solid tumors, drives tumorigenesis. The unambiguous answer is that not only can it do so (although perhaps not at the frequency that some models have predicted [Duesberg et al., 2004]), but it can also inhibit tumorigenesis and the cellular context is crucial. Both answers have important implications for human tumors.

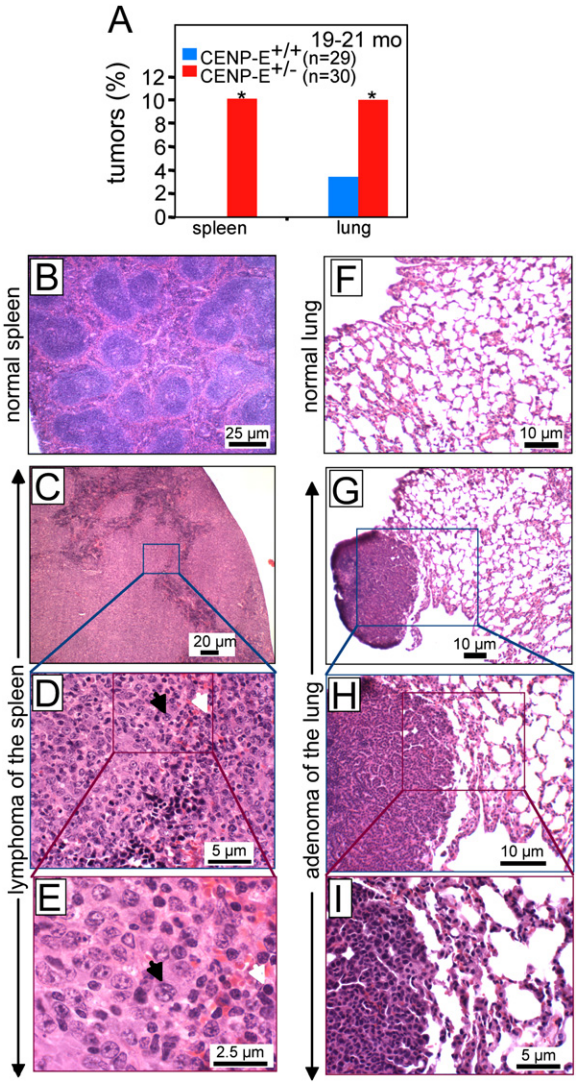

Figure 6. Aneuploidy Promotes Tumorigenesis
(A) Aged CENP-E$^{+/-}$ animals develop elevated levels of spontaneous spleen (p = 0.0402) and lung (p = 0.0492) tumors.
(B–I) H&E-stained tissue sections. (B) Normal spleen showing circular lymphoid follicles. (C–E) Lymphoma of the spleen showing effacement of lymphoid follicles and replacement of splenic architecture with a proliferation of neoplastic cells. (C) Box denotes region shown at higher magnification in (D). (D) Box denotes region shown at higher magnification in (E). Black arrow, neoplastic cell. White arrow, normal cell. (E) Neoplastic cell (black arrow, same cell as in [D]) with a high nucleus-to-cytoplasm ratio, an enlarged nucleus, and a prominent nucleolus. Normal cells (white arrow, same cell as in [D]) have dense, compact nuclei with very little cytoplasm. (F) Normal lung tissue exhibiting a lacy appearance. (G–I) Pulmonary adenoma of the lung. (G) Box denotes region shown at higher magnification in (H). (H) Enlargement of the border between the adenoma and the normal tissue, showing the glandular appearance of the adenoma. Box denotes region shown at higher magnification in (I). (I) Higher-magnification view of the delineated border between the adenoma and the adjacent normal tissue.

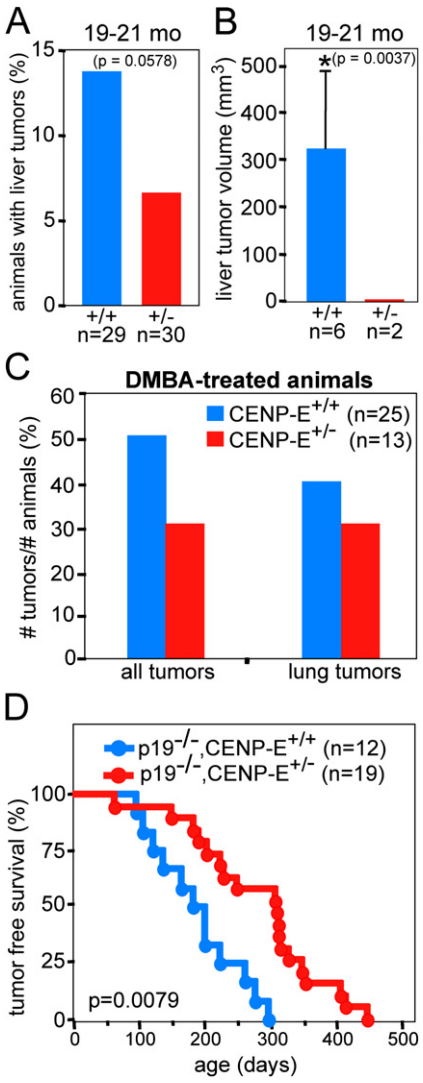

Figure 7. Aneuploidy Inhibits Tumorigenesis

(A) Aged CENP-E$^{+/-}$ animals have a decreased rate of spontaneous liver tumorigenesis.

(B) Liver tumors in CENP-E$^{+/-}$ animals are significantly smaller than those found in CENP-E$^{+/+}$ animals (p = 0.0037).

(C) CENP-E heterozygosity inhibits tumorigenesis in animals treated with the carcinogen DMBA.

(D) Aneuploidy due to CENP-E heterozygosity delays tumorigenesis in p19/ARF null mice.

Consistent with human cancers, aneuploidy-induced transformation is a slow process with a long latency, requiring ≥30 passages in culture. Even then it is not completely penetrant. Only a proportion of p19/ARF$^{-/-}$, CENP-E$^{+/-}$ cell lines acquired the ability to grow in soft agar and to form tumors in nude mice, even after ≥40 passages in culture. This apparently required the complex aneuploidy of the type routinely seen in solid human tumors. In animals, tumorigenesis was a late event, identified only in aged animals (19–21 months) and not in all tissues.

An additional insight from analysis of mice with markedly enhanced levels of whole-chromosomal aneuploidy is that CENP-E-deficient animals were remarkably normal despite high levels of aneuploidy. In light of the widely held presumption that the vast majority of cells in mammals in vivo are diploid, it is remarkable that organ development and function were relatively unimpaired, with little influence on normal growth, fertility, and life span (Figures S5B–S5D). These findings also reinforce the pioneering results of Chun and colleagues demonstrating that normal mice contain significant levels of single-chromosomal aneuploidy both in developing and adult neurons (Kaushal et al., 2003; McConnell et al., 2004; Rehen et al., 2001; Yang et al., 2003). Those authors have now extended this work to show that these aneuploid neurons are functional (Kingsbury et al., 2005). All of this challenges the assumption of a requirement for strict diploidy in mammals.

A further unexpected finding is that whole-chromosomal aneuploidy in vivo is characterized by a disproportionate number of examples of loss relative to gain (Figures 5A–5D). While it might be anticipated that chromosome losses would be more detrimental to cellular survival than gains, and hence would be underrepresented, the bias toward chromosome loss was observed uniformly in every experiment. Peripheral blood cells from animals from 2 to 20 months, as well as splenocytes from 8-month-old animals, all displayed substantially higher proportions of cells with fewer than a diploid complement of chromosomes than those with greater than 2n. This bias has also been seen in spontaneous aneuploidy in developing neurons (Kaushal et al., 2003; McConnell et al., 2004; Rehen et al., 2001; Yang et al., 2003) as well as in cells heterozygous for *Mad2* (Michel et al., 2001) and in embryos expressing a mutant version of the breast cancer gene *BRCA1* (Shen et al., 1998). Cells from mice heterozygous for BubR1 were also found to exhibit more losses than gains (Rao et al., 2005), although this difference was not observed in an independently created line (Baker et al., 2004). One possibility for this tendency toward chromosome loss is that lagging chromosomes in anaphase (produced by incorrect initial attachment or maintenance of that attachment) may be excluded from both daughter cells during cytokinesis. Alternatively, it may be that gain of most chromosomes results in increased levels of components that trigger senescence or apoptotic responses, thereby eliminating those cells from the cycling pool.

Aneuploidy has been argued to drive tumorigenesis (Li et al., 1997), to promote tumor progression but not initiation (Marx, 2002), and to be completely benign (Hahn et al., 1999). Since, to our knowledge, aneuploidy has never been proposed to inhibit tumorigenesis, this was our most surprising finding. Previous experiments did not uncover a role for aneuploidy in inhibiting tumorigenesis, even in animals with reduced levels of other proteins (Mad2, Bub3, and BubR1) that, like CENP-E, participate in the mitotic checkpoint. However, as detailed earlier, unlike CENP-E, these proteins are expressed throughout the cell cycle and have been implicated in apoptosis (BubR1), transcriptional repression (Bub3), the DNA

replication checkpoint (Mad2), and gross chromosomal rearrangements (Mad2, Bub3, BubR1). Consistent with this, Mad2 and BubR1 are expressed in differentiated tissues, while CENP-E is found only in tissues with a high proportion of dividing cells, such as testes and spleen (Figure S1C). Additionally, Mad2 and Bub3 mRNAs are expressed in postmitotic cells of the brain, while CENP-E mRNA is not (Allen Brain Atlas, http://www.brain-map.org/). Therefore, reduction of Mad2, Bub3, or BubR1 would be anticipated to produce defects in addition to simple increases in whole-chromosome aneuploidy that might affect their tumor-suppressing potential.

How can whole-chromosomal aneuploidy drive tumor suppression? Several factors probably converge to produce aneuploidy-mediated tumor inhibition. High levels of chromosomal instability can prevent clonal expansion, since cells that have acquired a rare transformative karyotype through multiple chromosome missegregations are likely to lose that karyotype in the next round of cell division. This situation is analogous to what has been shown for chromosome missegregation in bacteria. While low levels of instability provide a growth advantage, higher levels of instability generate a so-called ''mutational meltdown'' in which the population of highly aneuploid bacteria loses viability (Lynch et al., 1993). Such sensitivity is also analogous to genetic instability due to DNA damage. Cells sustain low levels of DNA damage on a regular basis, but this is normally countered by repair mechanisms. Higher levels of DNA damage due to mutations in mismatch repair enzymes result in viable cells but are associated with cancers, particularly hereditary nonpolyposis colorectal cancer (HNPCC; Strate and Syngal, 2005). Chemotherapeutic drugs (e.g., cisplatin) produce even higher levels of DNA damage, provoking cellular death and tumor regression. Our evidence now demonstrates that aneuploidy behaves similarly: it both drives tumorigenesis, as Boveri had initially proposed, and inhibits tumorigenesis, depending on the level of genomic damage that is induced.

EXPERIMENTAL PROCEDURES

Cell Culture

Primary MEFs were generated from day E14.5 embryos as described (http://medicine.wustl.edu/~escore/htmldocs/protocol.htm). Primary MEFs were grown in DMEM supplemented with 15% FBS, 0.1 mM nonessential amino acids (Gibco), 1 μM 2-mercaptoethanol (Specialty Media), 1 mM sodium pyruvate (Gibco), 2 mM glutamine, and 50 μg/ml pen/strep in a 37°C humidified incubator with 10% CO_2 and 3% oxygen. Low-oxygen conditions were used to extend the cycling time of the primary cells (Parrinello et al., 2003). p19/ARF null cells were grown in the same medium as primary MEFs in a 37°C humidified incubator with 7.5% CO_2 in atmospheric oxygen. MEFs immortalized with SV40 large T were grown in DMEM supplemented with 10% FBS, 2 mM glutamine, and 50 μg/ml pen/strep in a 37°C humidified incubator with 5% CO_2 and atmospheric oxygen.

Chromosome Spreads/Metaphase Spreads

Chromosome spreads from lymphocytes from peripheral blood were performed according to a Jackson Laboratory protocol (http://www.jax.org/cyto/blood_preps.html). Briefly, 200 μl heparinized blood obtained from ocular bleeds was added to 950 μl RPMI containing 100 μg/ml gentamycin, 100 μl 112 μg/ml PHA, 100 μl 750 μg/ml LPS, and 150 μl FBS. Cultures were incubated for 1.5 days at 37°C before 150 μl of 50 μg/ml colchicine was added and the cultures were incubated for an additional 4 hr. Cells were pelleted, gently resuspended in 2–3 ml 75 mM KCl prewarmed to 37°C, and incubated for 15 min at 37°C. Cells were pelleted and resuspended in a residual volume of ~250 μl, and then 3 ml fresh fix (3:1 methanol: acetic acid) was added dropwise while the tubes were vortexed at low speed. Cells were fixed at 4°C overnight. Spreads were made as specified below. To account for artifacts generated by the time in culture, aneuploidy measurements were corrected for the amount of aneuploidy observed in the youngest wild-type cells analyzed (~10% in 2-month-old animals).

Chromosome spreads from splenocytes were made by mincing freshly harvested spleens with forceps, washing the cells with PBS, resuspending in the same medium as above (including colchicine), and incubating at 37°C overnight. Cells were then harvested as above, except they were incubated in room-temperature KCl for 30 min.

Cultured cells were grown to ~80% confluence in 10 cm dishes. Cells were arrested in mitosis with 100 ng/ml colcemid for ~5 hr. Cells (including the less-adherent mitotic cells in the medium) were pelleted and resuspended in 3–5 ml 75 mM KCl for 10 min at room temperature. Five drops of fresh fix were added before the cells were pelleted again. Cells were resuspended in a residual volume of ~250 μl, and 3–5 ml fix was added dropwise while the tube was vortexed at low speed. Cells were fixed at 4°C overnight.

Just before spreads were made, cells were washed twice with fresh fix and resuspended in a small volume (~100–250 μl). To prepare spreads, 100 μl of cells was dropped onto a precleaned microscope slide, which was dried slowly for 10 s in a fume hood and dried quickly on an 80°C hot plate for 30 s. DNA was visualized with DAPI.

SKY was performed as described previously (Bowen et al., 2005).

FISH

Paraffin sections (6 μm thick) were adhered to glass slides and immersed in xylene for 2 × 20 min, and then for 1 min each in 100%, 85%, and 70% ethanol. Slides were washed in running tap water and immersed in ddH_2O before being pretreated with 0.2 N HCl for 20 min, washed in ddH_2O for 3 min, incubated in 8% sodium thiocyanate for 30 min at 80°C, washed in 2× SSC for 3 min, and digested in 0.5% pepsin in 0.2 N HCl for 1 hr at 37°C. Slides were washed in ddH_2O for 1 min and in 2× SSC for 5 min and then dehydrated for 1 min each in 70%, 85%, and 100% ethanol. Slides were dried in a 45°C oven before being denatured in 70% formamide in 2× SSC at 55°C for 40 s. Denatured slides were placed in ice-cold 70% ethanol and then room temperature 70%, 90%, and 100% ethanol for 3 min each. Slides were then air dried. Star*FISH whole-chromosome paint probes (Open Biosystems) were contemporaneously denatured by incubation for 10 min at 80°C and 30 min at 37°C and then applied to dried slides, before a coverslip was added and sealed with rubber cement. Slides were incubated overnight at 37°C in a humidified chamber and then washed for 5 min 2× in 50% formamide in SSC, 2× in SSC, and 1× for 3 min in 4× SSC + 0.05% Tween 20, all at 45°C. Cells were stained with DAPI and FM4-64 for 5 min before being washed with PBS and mounted using Prolong. Image stacks were acquired on a Nikon Eclipse TE 2000-E inverted spinning disk confocal microscope and flattened into a maximal projection before being scored. Both gains and losses of chromosomes were counted.

Transformation Assays

Focus formation assays were performed by plating cells in 6-well plates and allowing them to grow to confluence. Confluent cells were washed with PBS, fixed with methanol for 30 min, washed with PBS, and stained with 0.05% crystal violet for 30 min at room temperature before being washed with PBS and allowed to dry.

Soft agar assays were performed by plating 1 ml (2 ml for primary MEFs) of a 1:1 mix of 2× media and 1.2% agar per well of a 12-well

plate. Cells (2.5×10^5) in a 1:1 mix of 2× media and 0.6% agar were layered on top of the bottom agar after it solidified.

Nude mice injection experiments were performed by subcutaneously injecting 5×10^6 cells in PBS into 4- to 5-week-old nude mice. All experiments were performed in accordance with standards established by the Institutional Animal Care and Use Committee at UCSD.

Tumor Analysis and Histology

Aged animals were sacrificed by cervical dislocation following anesthetization with isofluorine. Necropsies were performed, and tissues as well as tumors observed by gross inspection were fixed in 10% formalin overnight at room temperature and then stored at 4°C before being embedded in paraffin. Hematoxylin-and-eosin-stained, 5 μm thick sections were prepared by the UCSD histology core and analyzed by Dr. Nissi Varki.

Supplemental Data

The Supplemental Data include six supplemental figures, one supplemental table, and one supplemental movie and can be found with this article online at http://www.cancercell.org/cgi/content/full/11/1/25/DC1/.

ACKNOWLEDGMENTS

The authors would like to thank Dr. Nissi Varki and the UCSD histology core, Janet Folmer (Johns Hopkins), and Dr. Dwayne Breining from the Department of Pathology (AECOM, Bronx, NY) for preparation and analysis of histological specimens. We would also like to thank Dr. James Feramisco and the UCSD Cancer Center microscopy facility. This work was supported by a National Institutes of Health grant to D.W.C. (GM29513). B.A.A.W. was supported, in part, by a postdoctoral fellowship from Philip Morris USA Inc. and Philip Morris international. Salary support for D.W.C. was provided by the Ludwig Institute for Cancer Research.

Received: July 14, 2006
Revised: October 26, 2006
Accepted: December 4, 2006
Published online: December 28, 2006

REFERENCES

Babu, J.R., Jeganathan, K.B., Baker, D.J., Wu, X., Kang-Decker, N., and van Deursen, J.M. (2003). Rae1 is an essential mitotic checkpoint regulator that cooperates with Bub3 to prevent chromosome missegregation. J. Cell Biol. *160*, 341–353.

Baek, K.H., Shin, H.J., Jeong, S.J., Park, J.W., McKeon, F., Lee, C.W., and Kim, C.M. (2005). Caspases-dependent cleavage of mitotic checkpoint proteins in response to microtubule inhibitor. Oncol. Res. *15*, 161–168.

Baker, D.J., Jeganathan, K.B., Cameron, J.D., Thompson, M., Juneja, S., Kopecka, A., Kumar, R., Jenkins, R.B., de Groen, P.C., Roche, P., and van Deursen, J.M. (2004). BubR1 insufficiency causes early onset of aging-associated phenotypes and infertility in mice. Nat. Genet. *36*, 744–749.

Baker, D.J., Jeganathan, K.B., Malureanu, L., Perez-Terzic, C., Terzic, A., and van Deursen, J.M. (2006). Early aging-associated phenotypes in Bub3/Rae1 haploinsufficient mice. J. Cell Biol. *172*, 529–540.

Boveri, T. (1902). Ueber mehrpolige Mitosen als Mittel zur Analyse des Zellkerns, English translation at. http://8e.devbio.com/article.php?ch=4&id=24. Vehr. d. phys. med. Ges. zu Wurzburg NF *35*, 67–90.

Boveri, T. (1914). Zur Frage der Entstehung maligner Tumoren (The Origin of Malignant Tumors) (Jena: Gustav Fischer).

Bowen, T.J., Yakushiji, H., Montagna, C., Jain, S., Ried, T., and Wynshaw-Boris, A. (2005). Atm heterozygosity cooperates with loss of Brca1 to increase the severity of mammary gland cancer and reduce ductal branching. Cancer Res. *65*, 8736–8746.

Brown, K.D., Coulson, R.M., Yen, T.J., and Cleveland, D.W. (1994). Cyclin-like accumulation and loss of the putative kinetochore motor CENP-E results from coupling continuous synthesis with specific degradation at the end of mitosis. J. Cell Biol. *125*, 1303–1312.

Campbell, M.S., Chan, G.K., and Yen, T.J. (2001). Mitotic checkpoint proteins HsMAD1 and HsMAD2 are associated with nuclear pore complexes in interphase. J. Cell Sci. *114*, 953–963.

Cleveland, D.W., Mao, Y., and Sullivan, K.F. (2003). Centromeres and kinetochores: From epigenetics to mitotic checkpoint signaling. Cell *112*, 407–421.

Dai, W., Wang, Q., Liu, T., Swamy, M., Fang, Y., Xie, S., Mahmood, R., Yang, Y.M., Xu, M., and Rao, C.V. (2004). Slippage of mitotic arrest and enhanced tumor development in mice with BubR1 haploinsufficiency. Cancer Res. *64*, 440–445.

Duesberg, P., Fabarius, A., and Hehlmann, R. (2004). Aneuploidy, the primary cause of the multilateral genomic instability of neoplastic and preneoplastic cells. IUBMB Life *56*, 65–81.

Fang, Y., Liu, T., Wang, X., Yang, Y.M., Deng, H., Kunicki, J., Traganos, F., Darzynkiewicz, Z., Lu, L., and Dai, W. (2006). BubR1 is involved in regulation of DNA damage responses. Oncogene *25*, 3598–3605.

Hahn, W.C., Counter, C.M., Lundberg, A.S., Beijersbergen, R.L., Brooks, M.W., and Weinberg, R.A. (1999). Creation of human tumour cells with defined genetic elements. Nature *400*, 464–468.

Hanks, S., Coleman, K., Reid, S., Plaja, A., Firth, H., Fitzpatrick, D., Kidd, A., Mehes, K., Nash, R., Robin, N., et al. (2004). Constitutional aneuploidy and cancer predisposition caused by biallelic mutations in BUB1B. Nat. Genet. *36*, 1159–1161.

Iouk, T., Kerscher, O., Scott, R.J., Basrai, M.A., and Wozniak, R.W. (2002). The yeast nuclear pore complex functionally interacts with components of the spindle assembly checkpoint. J. Cell Biol. *159*, 807–819.

Kalitsis, P., Fowler, K.J., Griffiths, B., Earle, E., Chow, C.W., Jamsen, K., and Choo, K.H. (2005). Increased chromosome instability but not cancer predisposition in haploinsufficient Bub3 mice. Genes Chromosomes Cancer *44*, 29–36.

Kamijo, T., Zindy, F., Roussel, M.F., Quelle, D.E., Downing, J.R., Ashmun, R.A., Grosveld, G., and Sherr, C.J. (1997). Tumor suppression at the mouse INK4a locus mediated by the alternative reading frame product p19ARF. Cell *91*, 649–659.

Kamijo, T., Bodner, S., van de Kamp, E., Randle, D.H., and Sherr, C.J. (1999). Tumor spectrum in ARF-deficient mice. Cancer Res. *59*, 2217–2222.

Kaushal, D., Contos, J.J., Treuner, K., Yang, A.H., Kingsbury, M.A., Rehen, S.K., McConnell, M.J., Okabe, M., Barlow, C., and Chun, J. (2003). Alteration of gene expression by chromosome loss in the postnatal mouse brain. J. Neurosci. *23*, 5599–5606.

Kim, M., Murphy, K., Liu, F., Parker, S.E., Dowling, M.L., Baff, W., and Kao, G.D. (2005). Caspase-mediated specific cleavage of BubR1 is a determinant of mitotic progression. Mol. Cell. Biol. *25*, 9232–9248.

Kingsbury, M.A., Friedman, B., McConnell, M.J., Rehen, S.K., Yang, A.H., Kaushal, D., and Chun, J. (2005). Aneuploid neurons are functionally active and integrated into brain circuitry. Proc. Natl. Acad. Sci. USA *102*, 6143–6147.

Li, R., Yerganian, G., Duesberg, P., Kraemer, A., Willer, A., Rausch, C., and Hehlmann, R. (1997). Aneuploidy correlated 100% with chemical transformation of Chinese hamster cells. Proc. Natl. Acad. Sci. USA *94*, 14506–14511.

Li, R., Sonik, A., Stindl, R., Rasnick, D., and Duesberg, P. (2000). Aneuploidy vs. gene mutation hypothesis of cancer: recent study claims mutation but is found to support aneuploidy. Proc. Natl. Acad. Sci. USA *97*, 3236–3241.

Lynch, M., Burger, R., Butcher, D., and Gabriel, W. (1993). The mutational meltdown in asexual populations. J. Hered. *84*, 339–344.

Mao, Y., Abrieu, A., and Cleveland, D.W. (2003). Activating and silencing the mitotic checkpoint through CENP-E-dependent activation/inactivation of BubR1. Cell *114*, 87–98.

Mao, Y., Desai, A., and Cleveland, D.W. (2005). Microtubule capture by CENP-E silences BubR1-dependent mitotic checkpoint signaling. J. Cell Biol. *170*, 873–880.

Marx, J. (2002). Debate surges over the origins of genomic defects in cancer. Science *297*, 544–546.

Matsuura, S., Matsumoto, Y., Morishima, K., Izumi, H., Matsumoto, H., Ito, E., Tsutsui, K., Kobayashi, J., Tauchi, H., Kajiwara, Y., et al. (2006). Monoallelic BUB1B mutations and defective mitotic-spindle checkpoint in seven families with premature chromatid separation (PCS) syndrome. Am. J. Med. Genet. A *140*, 358–367.

McConnell, M.J., Kaushal, D., Yang, A.H., Kingsbury, M.A., Rehen, S.K., Treuner, K., Helton, R., Annas, E.G., Chun, J., and Barlow, C. (2004). Failed clearance of aneuploid embryonic neural progenitor cells leads to excess aneuploidy in the Atm-deficient but not the Trp53-deficient adult cerebral cortex. J. Neurosci. *24*, 8090–8096.

McEwen, B.F., Chan, G.K., Zubrowski, B., Savoian, M.S., Sauer, M.T., and Yen, T.J. (2001). CENP-E is essential for reliable bioriented spindle attachment, but chromosome alignment can be achieved via redundant mechanisms in mammalian cells. Mol. Biol. Cell *12*, 2776–2789.

Michel, L.S., Liberal, V., Chatterjee, A., Kirchwegger, R., Pasche, B., Gerald, W., Dobles, M., Sorger, P.K., Murty, V.V., and Benezra, R. (2001). MAD2 haplo-insufficiency causes premature anaphase and chromosome instability in mammalian cells. Nature *409*, 355–359.

Myung, K., Smith, S., and Kolodner, R.D. (2004). Mitotic checkpoint function in the formation of gross chromosomal rearrangements in Saccharomyces cerevisiae. Proc. Natl. Acad. Sci. USA *101*, 15980–15985.

Parrinello, S., Samper, E., Krtolica, A., Goldstein, J., Melov, S., and Campisi, J. (2003). Oxygen sensitivity severely limits the replicative lifespan of murine fibroblasts. Nat. Cell Biol. *5*, 741–747.

Putkey, F.R., Cramer, T., Morphew, M.K., Silk, A.D., Johnson, R.S., McIntosh, J.R., and Cleveland, D.W. (2002). Unstable kinetochore-microtubule capture and chromosomal instability following deletion of CENP-E. Dev. Cell *3*, 351–365.

Quintanilla, M., Brown, K., Ramsden, M., and Balmain, A. (1986). Carcinogen-specific mutation and amplification of Ha-ras during mouse skin carcinogenesis. Nature *322*, 78–80.

Rao, C.V., Yang, Y.M., Swamy, M.V., Liu, T., Fang, Y., Mahmood, R., Jhanwar-Uniyal, M., and Dai, W. (2005). Colonic tumorigenesis in BubR1+/−ApcMin/+ compound mutant mice is linked to premature separation of sister chromatids and enhanced genomic instability. Proc. Natl. Acad. Sci. USA *102*, 4365–4370.

Rehen, S.K., McConnell, M.J., Kaushal, D., Kingsbury, M.A., Yang, A.H., and Chun, J. (2001). Chromosomal variation in neurons of the developing and adult mammalian nervous system. Proc. Natl. Acad. Sci. USA *98*, 13361–13366.

Rundell, K., and Parakati, R. (2001). The role of the SV40 ST antigen in cell growth promotion and transformation. Semin. Cancer Biol. *11*, 5–13.

Shen, S.X., Weaver, Z., Xu, X., Li, C., Weinstein, M., Chen, L., Guan, X.Y., Ried, T., and Deng, C.X. (1998). A targeted disruption of the murine Brca1 gene causes gamma-irradiation hypersensitivity and genetic instability. Oncogene *17*, 3115–3124.

Shin, H.J., Baek, K.H., Jeon, A.H., Park, M.T., Lee, S.J., Kang, C.M., Lee, H.S., Yoo, S.H., Chung, D.H., Sung, Y.C., et al. (2003). Dual roles of human BubR1, a mitotic checkpoint kinase, in the monitoring of chromosomal instability. Cancer Cell *4*, 483–497.

Strate, L.L., and Syngal, S. (2005). Hereditary colorectal cancer syndromes. Cancer Causes Control *16*, 201–213.

Sugimoto, I., Murakami, H., Tonami, Y., Moriyama, A., and Nakanishi, M. (2004). DNA replication checkpoint control mediated by the spindle checkpoint protein Mad2p in fission yeast. J. Biol. Chem. *279*, 47372–47378.

Wang, Q., Liu, T., Fang, Y., Xie, S., Huang, X., Mahmood, R., Ramaswamy, G., Sakamoto, K.M., Darzynkiewicz, Z., Xu, M., and Dai, W. (2004). BUBR1 deficiency results in abnormal megakaryopoiesis. Blood *103*, 1278–1285.

Weaver, B.A., Bonday, Z.Q., Putkey, F.R., Kops, G.J., Silk, A.D., and Cleveland, D.W. (2003). Centromere-associated protein-E is essential for the mammalian mitotic checkpoint to prevent aneuploidy due to single chromosome loss. J. Cell Biol. *162*, 551–563.

Wood, K.W., Sakowicz, R., Goldstein, L.S., and Cleveland, D.W. (1997). CENP-E is a plus end-directed kinetochore motor required for metaphase chromosome alignment. Cell *91*, 357–366.

Yang, A.H., Kaushal, D., Rehen, S.K., Kriedt, K., Kingsbury, M.A., McConnell, M.J., and Chun, J. (2003). Chromosome segregation defects contribute to aneuploidy in normal neural progenitor cells. J. Neurosci. *23*, 10454–10462.

Yen, T.J., Compton, D.A., Wise, D., Zinkowski, R.P., Brinkley, B.R., Earnshaw, W.C., and Cleveland, D.W. (1991). CENP-E, a novel human centromere-associated protein required for progression from metaphase to anaphase. EMBO J. *10*, 1245–1254.

Yoon, Y.M., Baek, K.H., Jeong, S.J., Shin, H.J., Ha, G.H., Jeon, A.H., Hwang, S.G., Chun, J.S., and Lee, C.W. (2004). WD repeat-containing mitotic checkpoint proteins act as transcriptional repressors during interphase. FEBS Lett. *575*, 23–29.

Yucel, J.K., Marszalek, J.D., McIntosh, J.R., Goldstein, L.S., Cleveland, D.W., and Philp, A.V. (2000). CENP-meta, an essential kinetochore kinesin required for the maintenance of metaphase chromosome alignment in Drosophila. J. Cell Biol. *150*, 1–11.

Zimonjic, D., Brooks, M.W., Popescu, N., Weinberg, R.A., and Hahn, W.C. (2001). Derivation of human tumor cells in vitro without widespread genomic instability. Cancer Res. *61*, 8838–8844.